Direct Observation of Two-Dimensional Magnetopolarons in a Resonant Tunnel Junction

G. S. Boebinger, A. F. J. Levi, S. Schmitt-Rink, A. Passner, L. N. Pfeiffer, and K. W. West
AT&T Bell Laboratories, Murray Hill, New Jersey 07974
(Received 28 February 1990)

Inelastic resonant tunnel spectroscopy is used to directly probe the density of states of two-dimensional magnetopolarons in a GaAs quantum well over a wide range of energies and magnetic fields. In agreement with theory, Landau levels are found to be drastically renormalized near degeneracies between the longitudinal-optic-phonon and cyclotron energies.

PACS numbers: 71.38.+i, 72.10.Di, 73.40.Kp

Electron tunneling in the presence of phonons gives rise to a number of interesting effects.[1] For example, LO-phonon-assisted resonant tunneling in GaAs is known to open up extra channels for current flow.[2] In polar semiconductors, such as GaAs, electrons interact with LO phonons to form polarons, i.e., the bare electron states are renormalized. In a resonant tunnel junction (Fig. 1), each confined two-dimensional electron subband is broadened and shifted to a new energy. If a magnetic field B is applied perpendicular to the plane of the barriers, the energy levels are further quantized into Landau levels of index n, both for elastic and phonon-assisted resonant tunneling.[3-5] The resulting magnetopolarons can exhibit dramatic renormalizations[6] which may be measured experimentally by monitoring the current-voltage characteristic of a resonant tunnel junction for different values of B. In this Letter, we use this technique as a spectroscopic tool to probe the density of states of two-dimensional magnetopolarons.

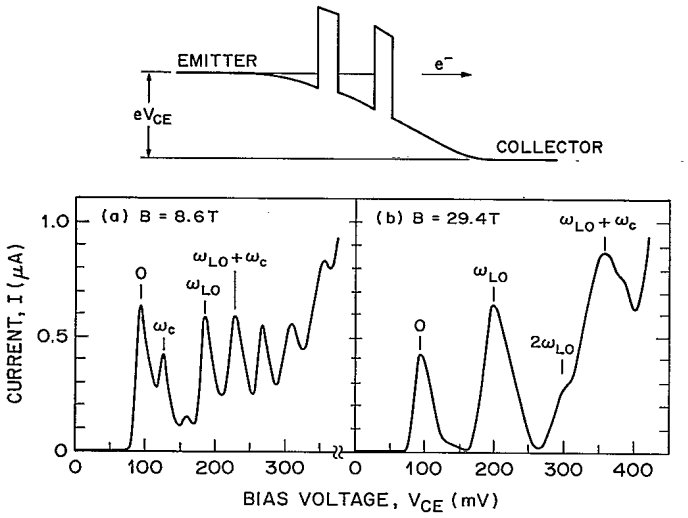

FIG. 1. Measured I_C-V_{CE} for a resonant tunnel structure with 30-Å-thick AlAs barriers and a 100-Å GaAs well. (a) $\omega_C < \omega_{LO}$, showing three resonance peaks in the current due to elastic tunneling and five peaks due to one LO-phonon-assisted tunneling. (b) $\omega_C > \omega_{LO}$, showing elastic, one and two LO-phonon-assisted tunneling. Note that bistability of the "0" resonance (not shown here) precludes determination of its true spectral weight (Ref. 7). Above is a schematic diagram of the conduction-band minimum for a resonant tunnel structure under bias, V_{CE}.

Double-barrier resonant tunnel structures (Fig. 1) are grown on ⟨100⟩-oriented GaAs substrates at 640 °C by molecular-beam epitaxy. An 8000-Å n-type (1×10^{18}-cm^{-3} Si impurities) GaAs collector contact is deposited on the substrate. This is followed by a ~500-Å undoped GaAs setback layer, grown to ensure minimal diffusion of Si impurities into the double-barrier structure. Of the various double-barrier structures grown, those discussed here consist of a symmetric pair of either 30- or 40-Å-thick AlAs barriers separated by a 100-Å GaAs well. The relatively narrow quantum well ensures that only resonances arising from the lowest-energy subband are observed in our experiments. Crystal growth is completed by growing a 100-Å GaAs setback layer and a 4000-Å $n=1\times10^{18}$ emitter contact. After removal from the growth chamber, the wafers are etched into ~90-μm-diam mesas and separate Ohmic contacts are made to the emitter and collector. The resonant tunneling current-voltage characteristics (I_C-V_{CE} traces) are tested at a temperature $T=0.3$ K in static (dc) magnetic fields up to $B=15$ T applied parallel to the direction of current flow through the tunnel structure.

For all data presented herein, the samples are placed in the bore of a solenoid capable of delivering a $B=50$ T sinusoidal pulse of ~5-ms duration. For each pulse of the magnet, one I_C-V_{CE} trace at $T=4.2$ K is measured at peak magnetic field (Fig. 1) during which time the magnetic field remains constant within a few percent. Sample current is detected by a series resistor located outside the magnetic field and data are collected by a 12-bit, 4-MHz transient digitizer. For each sample, the pulse magnetic-field data below $B=15$ T duplicate the results of measurements taken using a dc magnet.

All samples exhibit previously reported intrinsic bistability (see, e.g., Ref. 7) which results from a space charge as electrons accumulate in the quantum well. This bistability is enhanced in high magnetic fields and many resonances are observable only as V_{CE} decreases.[7] Thus, we only present I_C-V_{CE} data with decreasing V_{CE}.

(This also minimizes distortion of the spectra resulting from the charge buildup in the well.) Sweeping V_{CE} changes the energy difference between the two-dimensional emitter states and quantum well states. In zero magnetic field, two resonances are observed: at $V_{CE}=90$ mV for tunneling through the emitter barrier into the lowest-energy quantum well state and at $V_{CE}=200$ mV for tunneling by emitting a LO phonon of energy ω_{LO}. At $V_{CE}\gtrsim 280$ mV, the collector barrier is sufficiently lowered that the collector current I_C increases dramatically.

In a magnetic field applied parallel to the current (i.e., perpendicular to the plane to the barriers), the lowest-energy emitter and quantum well states are quantized into Landau levels with bare energy $E_n=(n+\frac{1}{2})\omega_C$, where $n=0,1,2,\ldots$ is the Landau-level index and $\omega_C=eB/m^*c$ is the cyclotron energy. In the absence of disorder or imperfections, inter-Landau-level tunneling is forbidden. However, emission of a LO phonon breaks this $\Delta n=0$ selection rule. This is illustrated in the I_C-V_{CE} trace of Fig. 1(a) in which are visible both the elastic ($\Delta n=0$) tunneling resonance (labeled "0" in the figure) and a series of strong resonances corresponding to single LO-phonon-assisted inter-Landau-level tunneling for $\Delta n=0$ ("ω_{LO}"), 1 ("$\omega_{LO}+\omega_C$"), 2, 3, and 4. Weaker resonances are observed which correspond to dissallowed $\Delta n=1$ ("ω_C") and 2 elastic (no LO-phonon emission) inter-Landau-level tunneling. These weaker peaks arise most likely from symmetry-breaking fluctuations in barrier thickness.[8] In Fig. 1(b), ω_C at $B=29.4$ T is larger than ω_{LO}. In this case, since the I_C-V_{CE} trace is no longer dominated by inter-Landau-level tunneling, the resonance for two-phonon emission ("$2\omega_{LO}$") becomes visible.

Figure 2 contains the resonance positions for each I_C-V_{CE} trace taken from the 30-Å barrier sample in pulsed magnetic fields to $B=44$ T. The three sizes of circles are proportional to the relative strengths of the peaks in the I_C-V_{CE} trace. At low magnetic fields, two Landau fans are readily discerned. The fan at lower voltage bias radiates from the elastic tunneling resonance at $V_{CE}=90$ mV and contains lines for $\Delta n=0$, 1, and 2. Since these $\Delta n\neq 0$ elastic transitions are extrinsic phenomena, they are denoted by open circles and are of secondary interest. The other Landau fan originates from the one LO-phonon-assisted resonance at $V_{CE}=200$ mV and transitions for $-1\leq\Delta n\leq 5$ are visible. The $\Delta n=-1$ transition disappears when the magnetic field depopulates the emitter $n=1$ Landau level. We attribute the observed parabolic distortion in the magnetic-field dependence of the inter-Landau-level transitions to increased depletion in the collector at high V_{CE}. At the top and right-hand side of Fig. 2, the natural magnetic field and energy scales are indicated. These are determined by scaling V_{CE} with known cyclotron energies at low-magnetic fields,[4] yielding a calculated LO-phonon energy of 37 meV for $\Delta V_{CE}\sim 110$ mV, in good agreement with the GaAs LO-phonon energy. The natural magnetic field

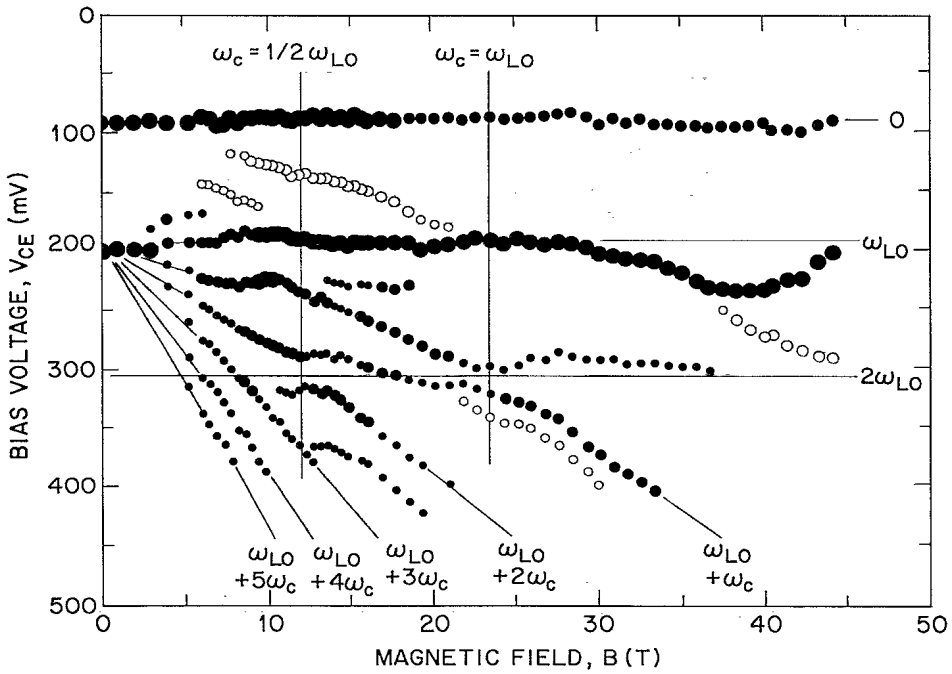

FIG. 2. Resonant tunneling peak positions vs magnetic field. The three circle sizes are proportional to the observed contribution to current (spectral weight). Open circles denote transitions forbidden except in the presence of (e.g., static) disorder. The natural energy and magnetic-field scales are given on the right-hand side and top. Note the anticrossings at the $2\omega_{LO}$ energy for $\omega_C=\frac{1}{2}\omega_{LO}$ and $\omega_C=\omega_{LO}$.

scale is set by $\omega_C=\omega_{LO}$ which occurs at around $B=23$ T in GaAs. (There is also some evidence in Fig. 2 of tunneling assisted by AlAs LO-phonon emission.[4] The roughly magnetic-field-independent line of points between ~ 13 and ~ 19 T at $V_{CE}\sim 230$ mV corresponds to an emission energy of 49 meV.)

The most striking features of the data in Fig. 2 are the two regions showing level anticrossing at the $2\omega_{LO}$ emission energy when $\omega_C=\omega_{LO}$ and $\omega_C=\frac{1}{2}\omega_{LO}$. In addition, at higher magnetic fields, the $(\omega_{LO}+n\omega_C)$ Landau fan shows clear evidence of being pinned to the $2\omega_{LO}$ energy. To understand the physics underlying these phenomena we have employed a simple theoretical model of LO-phonon-assisted resonant tunneling in a magnetic field. Our model relies on the transfer Hamiltonian formalism[1] which relates the current transmitted through a double-barrier resonant tunneling structure to the spectral function $A(n,E)$ of the bound state in the quantum well, i.e., to the probability of finding a bound electron in Landau level n with energy E. (Here and in the following, we only consider the lowest bound state.) The spectral function $A(n,E)$ is in turn determined by the imaginary part of the retarded Green's function $G(n,E)$ through

$$A(n,E)=-2\,\mathrm{Im}G(n,E)$$
$$=-2\,\mathrm{Im}[E-E_n+i\Gamma-\Sigma(n,E)]^{-1}, \qquad (1)$$

where $\Sigma(n,E)$ is the retarded self-energy due to interaction with LO phonons and Γ is a phenomenological broadening that accounts for the lifetime of the resonant state. For strong magnetic fields, it may readily be shown that the transmitted current is proportional to $A(0,E+E_0)$, where E is the zero-field detuning of the bound state with respect to the emitter. Thus, the transmitted current directly maps out the bound-state density of states projected onto the lowest $n=0$ Landau level.

At zero temperature and in the noncrossing (Migdal) approximation, the retarded self-energy describing multiple LO-phonon emission is given by

$$\Sigma(n,E)=\sum_{q,n'}|M_{n,n'}(q)|^2G(n',E-\omega_{LO}), \qquad (2)$$

where $M_{n,n'}(q)$ is the bound-state LO-phonon scattering matrix element, the strength of which may be characterized by the polaron coupling constant $\alpha=e^2(1/\epsilon_\infty-1/\epsilon_0)(m^*/2\omega_{LO})^{1/2}$, where ϵ_∞ and ϵ_0 are the high- and low-frequency dielectric constants, respectively. Equation (2) is of the form of a continued fraction expansion and becomes exact in the weak-coupling limit $\alpha\ll 1$. Its on-shell behavior has already been discussed in the literature.[6] We evaluated it numerically off the energy shell for $\alpha=0.1$ and $\Gamma=0.1\omega_{LO}$. For ease of computation, we assumed that strictly two-dimensional electron states exist in the well.

The basic scattering process described by Eq. (2) is one in which an electron in Landau level n with initial energy E is scattered into Landau level n' by emitting a LO phonon. Consider the lowest Landau level $n=0$. In the absence of interaction with LO phonons, its spectral function Eq. (1) is a Lorentzian centered at the unperturbed energy $E=E_0=\frac{1}{2}\omega_C$. Virtual one-phonon emission leads to a renormalization of this elastic "quasiparticle" peak resulting in a small reduction in spectral weight and a small polaron shift.[6] (For sake of clarity, we ignore the latter in the text; it is, however, included in our numerical results shown in Fig. 3.) The missing

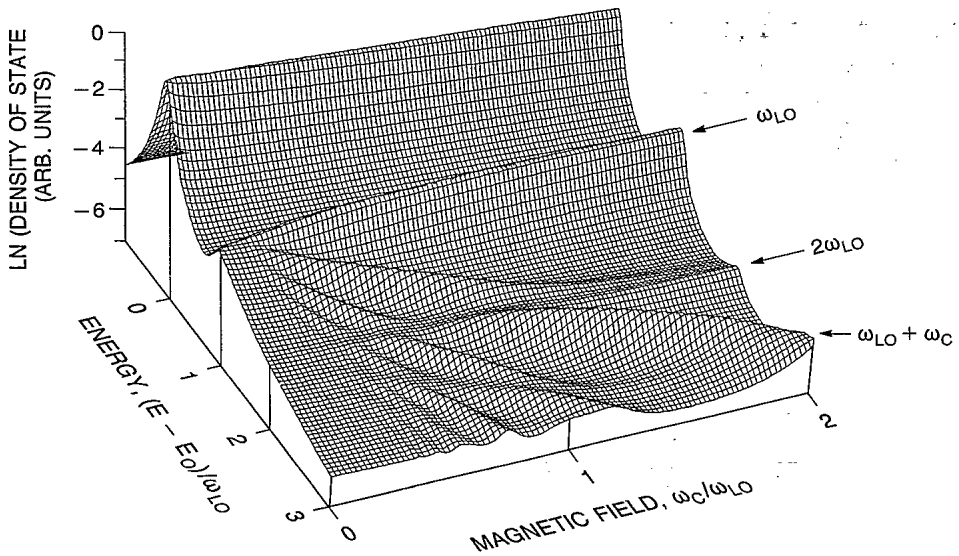

FIG. 3. Calculated natural logarithm of the two-dimensional magnetopolaron density of states projected onto the lowest Landau level. The energy E is measured from its unperturbed value $E_0=\frac{1}{2}\omega_C$ in units of the LO-phonon energy, ω_{LO}. Parameters used in the calculation were polaron coupling constant $\alpha=0.1$ and unperturbed energy-level broadening $\Gamma=0.1\omega_{LO}$.

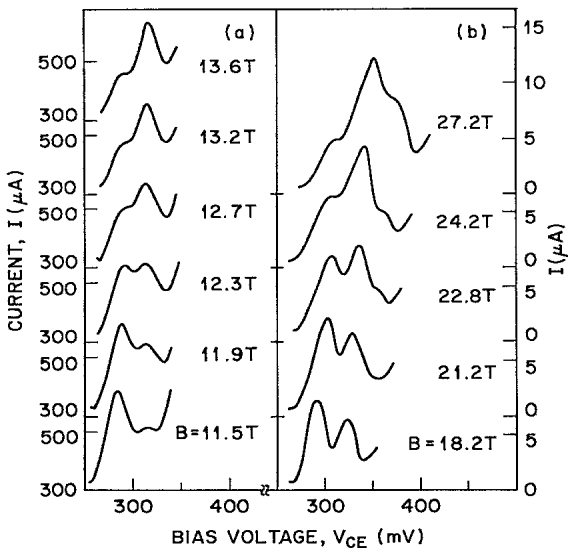

FIG. 4. Portions of I_C-V_{CE} traces near the anticrossings (a) at $\omega_C = \frac{1}{2}\omega_{LO}$ for the 30-Å barrier sample and (b) at $\omega_C = \omega_{LO}$ for the 40-Å barrier sample. Note the different current scales and zero offsets.

spectral weight appears in the form of inelastic "incoherent" (i.e., real one-phonon) excitations at energies $E \sim \omega_{LO} + E_{n'}$, which accounts for the Landau fan originating from the one-phonon resonance in Figs. 2 and 3. Two-phonon processes lead to a further (but much smaller) renormalization of the elastic quasiparticle peak and to a second Landau fan at energies $E \sim 2\omega_{LO} + E_{n''}$, which interferes with the first one. Degeneracies between the two Landau fans at $\omega_{LO} = E_{n'} - E_{n''} = (n' - n'')\omega_C$ are removed by the electron LO-phonon interaction which leads to energy-level anticrossing and pinning of Landau levels to multiples of LO-phonon energies. Both these effects are predicted theoretically (Ref. 6 and Fig. 3) and are clearly seen in our experiments (Fig. 2). For example, as magnetic field increases, the state labeled $\omega_{LO} + \omega_C$ (see Figs. 2 and 3) does not cross the $2\omega_{LO}$ state at the $\omega_C = \omega_{LO}$ resonances. Instead, there is an anticrossing and pinning to the $2\omega_{LO}$ energy at higher magnetic fields. Similarly, the $\omega_{LO} + 2\omega_C$ resonance at low magnetic fields anticrosses and becomes pinned at the $2\omega_{LO}$ energy for $B > 15$ T. The $2\omega_{LO}$ line then anticrosses to become the $\omega_{LO} + \omega_C$ line at the highest magnetic fields. Figure 4 contains portions of the I_C-V_{CE} traces for the anticrossings at $\omega_C = \frac{1}{2}\omega_{LO}$ and $\omega_C = \omega_{LO}$, showing the shift in spectral weight from one resonance to the other.

The theoretical spectral function reproduces the qualitative behavior of the experimental data remarkably well, despite the approximations made in our model. As an aside, the inclusion of elastic scattering[9] in our model qualitatively reproduces the $\Delta n = 1$ and 2 elastic (no LO-phonon emission) inter-Landau-level tunneling shown as open circles in Fig. 2.

In conclusion, we have used a resonant tunnel junction to directly probe the density of states of two-dimensional magnetopolarons by inelastic resonant tunnel spectroscopy. The measurements are in good qualitative agreement with a simple theoretical model and reveal for the first time Landau-level anticrossing and pinning behavior near LO-phonon and cyclotron energy degeneracies.

[1]L. I. Glazman and R. I. Shekhter, Zh. Eksp. Teor. Fiz. **94**, 292 (1988) [Sov. Phys. JETP **67**, 163 (1988)]; N. S. Wingreen, K. W. Jacobsen, and J. W. Wilkins, Phys. Rev. Lett. **61**, 1396 (1988); Phys. Rev. B **40**, 11834 (1989); B. Y. Gelfand, S. Schmitt-Rink, and A. F. J. Levi, Phys. Rev. Lett. **62**, 1683 (1989); W. Cai. T. F. Zheng, P. Hu, B. Yudanin, and M. Lax, Phys. Rev. Lett. **63**, 418 (1989); M. Jonson, Phys. Rev. B **39**, 5924 (1989).

[2]V. J. Goldman, D. C. Tsui, and J. E. Cunningham, Phys. Rev. B **36**, 7635 (1987).

[3]E. E. Mendez, L. Esaki, and W. I. Wang, Phys. Rev. B **33**, 2893 (1986).

[4]M. L. Leadbeater, E. S. Alves, L. Eaves, M. Henini, O. H. Hughes, A. Celeste, J. C. Portal, G. Hill, and M. A. Pate, Phys. Rev. B **39**, 3438 (1989).

[5]C. H. Yang, M. J. Yang, and Y. C. Kao, Phys. Rev. B **40**, 6272 (1989).

[6]S. Das Sarma, Phys. Rev. Lett. **52**, 859 (1984); **52**, 1570(E) (1984); D. M. Larsen, Phys. Rev. B **30**, 4807 (1984); F. M. Peeters and J. T. Devreese, Phys. Rev. B **31**, 3689 (1985).

[7]L. Eaves, M. L. Leadbeater, D. G. Hayes, E. S. Alves, F. W. Sheard, G. A. Toombs, P. E. Simmonds, M. S. Skolnick, M. Henini, and O. H. Hughes, Solid State Electron. **32**, 1101 (1989).

[8]J. Leo and A. H. MacDonald, Phys. Rev. Lett. **64**, 817 (1990).

[9]H. A. Fertig and S. Das Sarma, Phys. Rev. B **40**, 7410 (1989).